CALPHAD: Computer Coupling of Phase Diagrams and Thermochemistry 33 (2009) 478–486

Contents lists available at ScienceDirect

CALPHAD: Computer Coupling of Phase Diagrams and Thermochemistry

journal homepage: www.elsevier.com/locate/calphad

A critical thermodynamic assessment of the Mg–Ni, Ni–Y binary and Mg–Ni–Y ternary systems

Mohammad Mezbahul-Islam, Mamoun Medraj *

Department of Mechanical Engineering, Concordia University, 1455 de Maisonneuve Blvd. West, H3G 1M8, Montreal, Canada

ARTICLE INFO

Article history:
Received 19 August 2008
Received in revised form
5 January 2009
Accepted 5 January 2009
Available online 17 January 2009

Keywords:
Thermodynamic modeling
Modified quasichemical model
Mg-alloys
Hydrogen storage
Metallic glass

ABSTRACT

A thorough review and critical evaluation of phase equilibria and thermodynamic data for the phases in the Mg–Ni–Y ternary system have been carried out over the entire composition range from room temperature to above the liquidus. This system is being modeled for the first time using the modified quasichemical model which considers the presence of short range ordering in the liquid. The Gibbs energies of the different phases have been modeled, and optimized model parameters that reproduce all the experimental data simultaneously within experimental error limits have been obtained. For the liquid phases, the modified quasichemical model is applied. A sublattice model within the compound-energy formalism is used to take proper account of the structures of the binary intermediate solid solutions. The Mg–Ni and Ni–Y binary systems have been re-optimized based on the experimental phase equilibrium and thermodynamic data available in the literature. The optimized thermodynamic parameters for the Mg–Y system are taken from the previous thermodynamic assessment of the Mg–Cu–Y system by the same authors. The constructed database has been used to calculate liquidus projection, isothermal and vertical sections which are compared with the available experimental information on this system. The current calculations are in a good agreement with the experimental data reported in the literature.

1. Introduction

Batteries can be a useful source of energy for spacecraft, military and defense, communication, power tools and consumer appliances because of their ability to store energy in a clean, convenient and efficient manner and hence there is a growing need for high-specific power, high-specific energy and low-cost batteries [1]. Currently nickel/cadmium rechargeable batteries are commonly used for these purposes. But due to the relatively low capacity and environmental concerns more efficient and safe substitutes for cadmium are urgently needed. The nickel-metal hydride battery (MH) with a hydrogen storage alloy as a negative electrode has shown a high potential in that aspect [1,2]. That is why extensive attention has been paid to the utilization of magnesium-based alloys as hydrogen storage materials owing to their high storage capacity and low specific weight [3]. The Mg–Ni–Y system is considered to be one of the promising candidates [1]. Besides, this ternary is one of the promising Mg-based metallic glass systems [4]. Hence it is becoming clear that a detailed investigation on this system is needed.

The aim of the present work is to provide a comprehensive critical thermodynamic evaluation and optimization of the Mg–Ni–Y system over the entire composition range from room temperature to liquidus temperature. Two of the three constituent binaries, Mg–Ni and Ni–Y, have been optimized using the modified quasichemical model [5–7] for the liquid phase. The Mg–Y system was optimized earlier by the same authors [8] and the model parameters have been used directly in this work. The Toop [9] geometric model with Mg as the asymmetric component has been used for the extrapolation of the binaries to the ternary system.

2. Literature review

2.1. Ni–Y system

The phase diagram of the Ni–Y system was first investigated by Beaudry and Daane [10] and later by Domagala et al. [11]. Beaudry and Daane [10] used metallographic, thermal analysis and X-ray diffraction (XRD) methods in their investigation and reported the existence of nine intermetallic compounds; NiY_3, Ni_2Y_3, Ni_2Y, Ni_3Y, Ni_7Y_2, Ni_4Y, $Ni_{17}Y_2$, NiY and Ni_5Y. Except for the last two, all other compounds undergo peritectic decomposition. Domagala et al. [11], however, reported eight compounds and missed the existence of Ni_7Y_2. However, another investigation by Buschow [12] on several phases of the Ni–RE (RE = rare earth) showed that an Ni_7RE_2 phase occurs in all the heavier Ni–RE systems. So the existence of the Ni_7Y_2 compound in the Ni–Y system is consistent with the general trend and has been included in this work. Domagala et al. [11], also, disagreed

* Corresponding author.
E-mail address: mmedraj@encs.concordia.ca (M. Medraj).

0364-5916/$ – see front matter © 2009 Elsevier Ltd. All rights reserved.
doi:10.1016/j.calphad.2009.01.001

with Beaudry and Daane [10] about the stoichiometry of the most Ni-rich intermediate phase reporting the composition to be Ni_9Y not $Ni_{17}Y_2$. Studying the crystal structure data reported by Buschow [13] reveals that the stoichiometry should be $Ni_{17}Y_2$. This composition was also accepted by several other assessments [14–17] and hence it is used in the current analysis. The temperature and composition of the three eutectic reactions reported by [10,11] are consistent with each other and have been used in the current assessment with more weight for the data of [10] since the error associated with the data of [11] is higher.

Beaudry and Daane [10] reported the solubility of yttrium in nickel to be 0.1 at.% at 1523 K, while the solubility of nickel in yttrium to be 0.2 at.% at 1173 K. On the other hand, Domagala et al. [11] reported it to be less than 1 wt.% in either terminal solution. The value reported by [11] seems to be very high considering the mutual solubility between Ni and other rare earth metals [18–22]. Hence, it is decided to be consistent with the solubilities reported by [10].

The magnetic properties of the intermetallic compounds in the Ni–Y system were summarized by Buschow [12] and also by Gignoux et al. [23,24]. None of the Ni–Y compounds has a magnetic ordering temperature above room temperature. The highest value is found in the $Ni_{17}Y_2$ compound and is close to 160 K [12]. Also, Beaudry and Daane [10] did not find any of the intermetallic compounds to show magnetic behavior at room temperature. Hence the magnetic contribution is not added in the optimization of this system.

Not many works on the experimental thermodynamic properties of the Ni–Y system could be found in the literature. Subramanian and Smith [15] determined the enthalpy of formation of the nine intermediate phases using the electromotive force (emf) measurements over the temperature range of 900–1225 K. Estimations of the enthalpy of formation of these compounds were done by [25–27] but these values will not be used during optimization and only the experimentally measured values by Subramanian and Smith [15] will be used. Batalin et al. [28] measured the enthalpy of mixing of the liquid Ni–Y at 1973 K using differential thermal analysis (DTA). The present calculation will be compared with their results.

Thermodynamic assessments were done on the Ni–Y system by Nash [14], Du and Zhang [16] and Mattern et al. [17]. In spite of the high negative v-shaped experimental enthalpy of mixing data [28], none of these assessments considered the presence of short range ordering in the liquid. Therefore, it is decided to re-optimize the Ni–Y system using the modified quasichemical model which considers the presence of short range ordering in the liquid.

2.2. Mg–Ni system

Voss [29] was the first researcher who investigated the Mg–Ni system by thermal analysis in the composition range $0.04 < X_{Ni} < 0.98$. But in his work, the purity of Mg was not specified and the purity of Ni was low (97.7 wt%). Later, Haughton and Payne [30] determined the liquidus temperature more accurately in the Mg-rich end ($0 \leq X_{Ni} \leq 0.34$) by thermal analysis with high purity of elements. Bagnoud and Feschotte [31] investigated the system using XRD, metallography, EPMA and DTA. Micke and Ipser [32] determined the magnesium vapor pressure over the Mg–Ni liquid in the $X_{Mg} > 0.65$ composition range by the isopiestic method. They also obtained the liquidus curve between $0.30 < X_{Ni} < 0.40$. According to these investigations, there are two eutectic and one peritectic reactions in the Mg–Ni system. Two intermetallic compounds have been reported; Mg_2Ni melts incongruently (1033 K) and $MgNi_2$ melts congruently (1420 ± 3 K). Bagnoud and Feschotte [31] investigated the homogeneity range of $MgNi_2$ and mentioned that it extends from 66.2 at.% Ni to 67.3 at.% Ni. All these data are used in the optimization except a few data points of Voss [29] due to the lack of consistency with the entire phase diagram. Their data also deviate a lot from the reported experimental data points of other researchers [30,32].

Haughton and Payne [30] mentioned that the solid solubility of Ni in Mg is less than 0.04 at.% Ni at 773 K, whereas Merica and Waltenberg [33] reported that the solid solubility of Mg in Ni is less than 0.2 at.% Mg even at 1373 K. The abovementioned solubilities have been used in the present work. Wollam and Wallace [34] and Buschow [35] disputed the ferromagnetic behavior of this system. They investigated the system by heat capacity and magnetic susceptibility measurements and did not find any anomaly in these properties for $MgNi_2$ at any temperature. Hence the ferromagnetic behavior of Ni is not included in the current assessment.

Laves and Witte [36] determined the crystal structure of the Laves phase $MgNi_2$ to be hexagonal hP24-type with 8 molecules per unit cell, and the lattice parameters as $a = 0.48147$ and $c = 1.58019$ nm which are in a good agreement with the reported values of Lieser and Witte [37], and Bagnoud and Feschotte [31]. The crystal structure of Mg_2Ni was determined by Schubert and Anderko [38] who reported a hexagonal, C16-type structure with 6 molecules per unit cell and lattice parameters of $a = 0.514$ and $c = 1.322$ nm which agree with those reported by Buschow [35].

Feufel and Sommer [39] measured the integral enthalpy of mixing by the calorimetric method at 1002 K and 1008 K. Micke and Ipser [32] determined the activity of Mg at several temperatures using the isopiestic method. Reasonable agreement was found between their [32] results and those of Sryvalin et al. [40] in the composition range $X_{Ni} \leq 0.30$. Sieben et al. [41] also measured the activity of Mg from Mg vapor pressure.

Enthalpy of formation of the $MgNi_2$ and Mg_2Ni compounds were measured by Sieben et al. [41], Smith and Christian [42], King and Kleppa [43], and Lukashenko and Eremenko [44]. All these data are in reasonable agreement and will be compared with the current work.

Thermodynamic calculations of this system were carried out by Nayeb-Hashemi and Clark [45], Jacobs and Spencer [46] and most recently by Islam and Medraj [47]. But since we are using the modified quasichemical model for the liquid phase of the other two binaries, the Mg–Ni system needs to be re-optimized using this model.

2.3. Mg–Ni–Y ternary system

The isothermal section at 673 K of the Mg–Ni–Y system (Ni $\geq$ 50%) was investigated by Yao et al. [48] who confirmed the existence of two ternary compounds Mg_2Ni_9Y and $MgNi_4Y$ at 673 K. The compositions of these ternary compounds were reported earlier by Kadir et al. [49–51] and Aona et al. [52]. $MgNi_4Y$ has a cubic $SnMgCu_4$($AuBe_5$-type) structure, which is related to the (C_{15}) $MgCu_2$ structure [51]. Kadir et al. [50] reported a hexagonal structure for Mg_2Ni_9Y compound which is an isostructure of $LaMg_2Ni_9$ with AB_2C_9-type. However, the enthalpy of formation or melting temperature of these compounds has not been determined yet. Yao et al. [48] investigated the 673 K isothermal section of the Ni-rich region of the Mg–Ni–Y system using XRD, SEM and DTA. They reported 13 single-phase regions, 25 two-phase regions and 13 three-phase regions. A complete description of the equilibria in the Mg–Ni–Y system is still unknown.

3. Analytical descriptions of the employed thermodynamic models

The Gibbs energy function used for the pure elements i (i = Mg, Ni and Y) are taken from the SGTE (Scientific Group Thermodata Europe) compilation of Dinsdale [53].

The Gibbs energy of a binary *stoichiometric phase* is given by:

$$G^{\phi} = x_i {}^0G_i^{\phi_1} + x_j {}^0G_j^{\phi_2} + \Delta G_f \quad (1)$$

where ϕ denotes the phase of interest, x_i and x_j are mole fractions of elements i and j which are given by the stoichiometry of the compound, ${}^0G_i^{\phi_1}$ and ${}^0G_i^{\phi_2}$ are the respective reference states of elements i and j in their standard state and $\Delta G_f = a + bT$ represents the Gibbs energy of formation of the *stoichiometric compound*. The parameters a and b were obtained by optimization using experimental data.

The Gibbs energy for the *terminal solid solution phases* is described by the following equation:

$$G^{\phi} = x_i\,{}^0G_i^{\phi} + x_i\,{}^0G_j^{\phi} + RT[x_i \ln x_i + x_j \ln x_j] + {}^{ex}G^{\phi} \quad (2)$$

where ϕ denotes the phase of interest and x_i, x_j denote the mole fraction of components i and j, respectively. The first two terms on the right hand side of Eq. (2) represent the Gibbs energy of the mechanical mixture of the components, the third term is the ideal Gibbs energy of mixing, and the fourth term is the excess Gibbs energy, which is described by the Redlich–Kister polynomial model in this work and can be represented as:

$${}^{ex}G^{\phi} = x_i.x_j \sum_{n=0}^{n=m} {}^nL_{i,j}^{\phi}(x_i - x_j)^n \quad (3)$$

$${}^nL_{i,j}^{\phi} = a_n + b_n \times T \quad (4)$$

where a_n and b_n are the parameters of the model that need to be optimized considering the experimental phase diagram and thermodynamic data.

The modified quasichemical model [5–7] was chosen to describe the *liquid phases* of the three constituent binaries. From the literature survey, it was found that the binary systems especially the Ni–Y system has a very high negative enthalpy of mixing. This is an indication of the presence of short range ordering [5] in the liquid. Also it is observed that systems showing glass forming ability may have short range ordering in the liquid. Therefore, it is decided to consider the presence of short range ordering in the liquid while modeling the *liquid* phase since this Mg–Ni–Y system showed some glass forming ability [4]. The modified quasichemical model is the most suitable model to describe the short range ordering in the liquid. It has three distinct characteristics [8–10]: (i) It permits the composition of maximum short range ordering in a binary system to be freely chosen. (ii) It expresses the energy of pair formation as a function of composition which can be expanded as a polynomial in the pair fraction. Also, the coordination numbers are permitted to vary with the composition. (iii) The model can be extended to multicomponent systems. The model has been discussed extensively in the literature [5–7] and will be outlined briefly here. The energy of pair formation can be expressed by the following equation:

$$\Delta g_{AB} = \Delta g_{AB}^{o} + \sum_{i\geq 1} g_{AB}^{i0} X_{AA}^{i} + \sum_{j\geq 1} g_{AB}^{0j} X_{BB}^{j} \quad (5)$$

where Δg_{AB}^{o}, g_{AB}^{i0} and g_{AB}^{0j} are the parameters of the model and can be expressed as functions of temperature ($\Delta g_{AB}^{o} = a + bT$). Also, the atom to atom coordination number Z_A and Z_B can be expressed as a function of composition and can be presented by the following equations:

$$\frac{1}{Z_A} = \frac{1}{Z_{AA}^{A}}\left(\frac{2n_{AA}}{2n_{AA}+n_{AB}}\right) + \frac{1}{Z_{AB}^{A}}\left(\frac{n_{AB}}{2n_{AA}+n_{AB}}\right) \quad (6)$$

$$\frac{1}{Z_B} = \frac{1}{Z_{BB}^{B}}\left(\frac{2n_{BB}}{2n_{BB}+n_{AB}}\right) + \frac{1}{Z_{BA}^{B}}\left(\frac{n_{AB}}{2n_{BB}+n_{AB}}\right) \quad (7)$$

n_{ij} is the number of moles of $(i-j)$ pairs, Z_{AA}^{A} and Z_{AB}^{A} are the coordination numbers when all nearest neighbors of an A atom are A or B atoms, respectively. The composition of maximum short range ordering is determined by the ratio Z_{BA}^{B}/Z_{AB}^{A}. Values of Z_{AB}^{A} and Z_{BA}^{B} are unique to the A–B binary system and should be carefully determined to fit the thermodynamic experimental data (enthalpy of mixing, activity etc.). The selected values in the present work are given in Table 1. The tendency to maximum short range ordering near the composition 45 at.% Y in the Ni–Y system was obtained by setting $Z_{NiY}^{Ni} = 5$ and $Z_{NiY}^{Y} = 6$. For the Mg–Ni system, experimental enthalpy of mixing data are available only near the Mg-rich region. Following the trend of these data and studying previous optimization works on this system [45–47], it is assumed that the maximum short range ordering should be near 35 at.% Ni which was obtained by setting $Z_{MgNi}^{Mg} = 2$ and $Z_{MgNi}^{Ni} = 4$. The value of Z_{AA}^{A} is common for all systems containing A as a component. The same is true for all components. In this work, the value of Z_{MgMg}^{Mg}, Z_{NiNi}^{Ni} and Z_{YY}^{Y} was chosen to be 6 because it gave the best possible fit for many binary systems and is recommended by Dr. Pelton's group [5–7].

Table 1
Atom–atom "coordination numbers" of the liquid phase constituents.

A	B	Z_{AB}^{A}	Z_{AB}^{B}
Mg	Mg	6	6
Y	Y	6	6
Ni	Ni	6	6
Mg	Ni	2	4
Y	Ni	6	5

The Gibbs energy of intermediate solid solutions is described by the compound energy formalism as shown in the following equations:

$$G = G^{ref} + G^{ideal} + G^{excess} \quad (8)$$

$$G^{ref} = \sum y_i^l y_j^m \ldots y_k^q {}^0G_{(i,j,\ldots,k)} \quad (9)$$

$$G^{ideal} = R(T/K)\sum_l f_l \sum_l y_i^l \ln y_i^l \quad (10)$$

$$G^{excess} = \sum y_i^l y_j^l y_k^m \sum_{\gamma=0}^{\gamma} L_{(i,j,):k} \times (y_i^l - y_j^l)^{\gamma} \quad (11)$$

where $i, j, \ldots, k$ represent components or vacancy, l, m and q represent sublattices, y_i^l is the site fraction of component i on sublattice l, f_l is the fraction of sublattice l relative to the total lattice sites, ${}^0G_{(i:j:..k)}$ represents a real or a hypothetical compound (end member) energy, and ${}^{\gamma}L_{(i,j)}$ represents the interaction parameters which describe the interaction within the sublattice.

4. Results and discussion

All the calculations in this work have been done using the FactSage Software [54]. The calculated Ni–Y phase diagram along with the experimental data from [10,11] is shown in Fig. 1, which shows a good agreement with the experimental data of Beaudry and Daane [10]. Some melting temperature data of the compounds especially near the Ni-rich region (0.7–0.9 at.% Ni) disagreed with the data of Domagala et al. [11]. However it is decided to be consistent with the data of Beaudry and Daane [10] because Domagala et al. [11] determined the melting point of the compounds by visual analysis of the samples and reported relatively high error ±25 K in these measurements, whereas Beaudry and Daane [10] used thermal and metallographic methods and reported smaller error of ±5 K. In the current assessment, the mutual solubility between Y and Ni is considered very low based on the work of [10]. The optimized parameters of the liquid and intermetallic compounds are given in Table 2. The parameters for the Gibbs energy of formation for the compounds are given at room temperature.

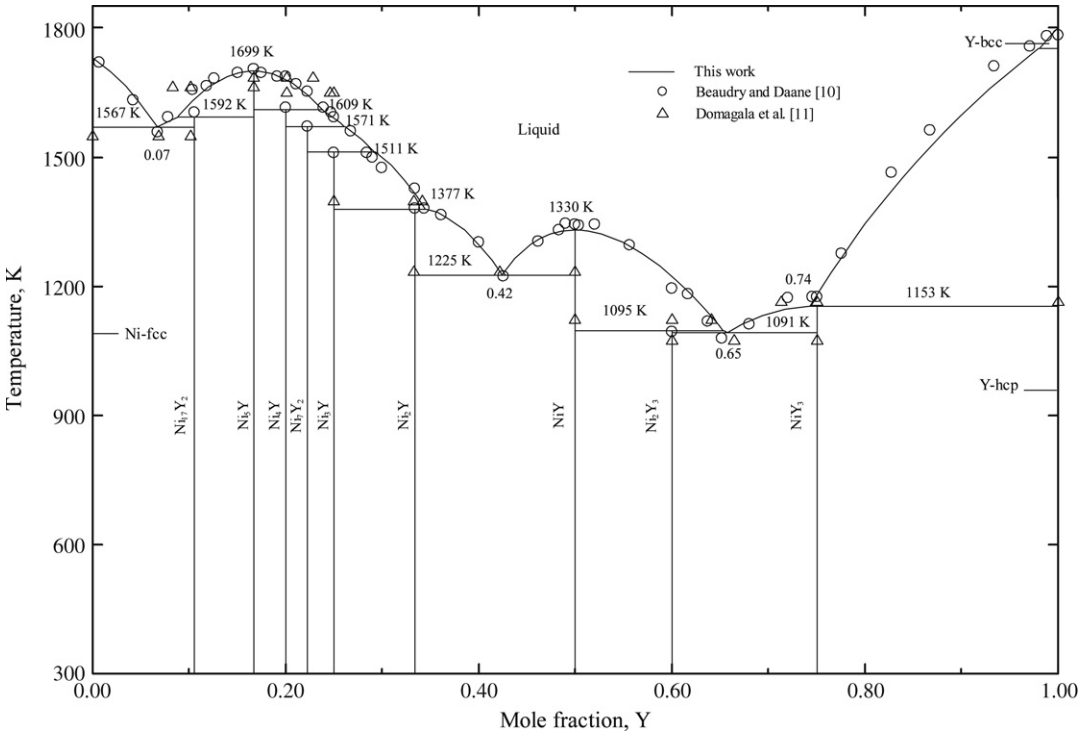

Fig. 1. Calculated Ni–Y phase diagram.

Table 2
Optimized model parameters of the Ni–Y system.

Phase	Terms	a (J/mol atom)	b (J/mol atom K)
Liquid	$\Delta g^{0}_{Y:Ni}$	−33,653.83	1.61
	$g^{Y:0}_{Y:Ni}$	−1,339.46	1.26
	$g^{Ni:0}_{Y:Ni}$	−17,538.50	0.00
Ni-fcc	${}^{0}L^{Ni\text{-}fcc}$	3,348.64	0.00
Y-bcc	${}^{0}L^{Y\text{-}bcc}$	418.58	0.00
Y-hcp	${}^{0}L^{Y\text{-}hcp}$	0	0.00
$Ni_{17}Y_2$	ΔG_f	−18,205.16	0.874
Ni_5Y	ΔG_f	−28,350.23	1.492
Ni_4Y	ΔG_f	−152,853.25	1.965
Ni_7Y_2	ΔG_f	−33,133.95	1.876
Ni_3Y	ΔG_f	−34,313.80	1.657
Ni_2Y	ΔG_f	−37,389.37	2.039
NiY	ΔG_f	−35,284.53	0.832
Ni_2Y_3	ΔG_f	−29,475.63	1.208
NiY_3	ΔG_f	−19,671.02	0.874

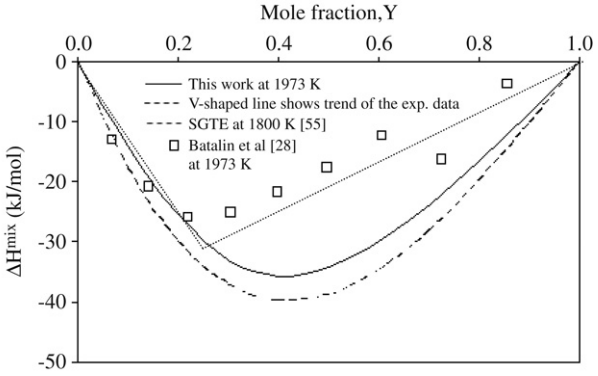

Fig. 2. Calculated enthalpy of mixing of liquid Ni–Y at 1973 K.

There is not enough experimental data on the thermodynamic properties of the liquid Ni–Y. The only available data is from Batalin et al. [28] who measured the integral enthalpy of mixing at 1973 K. The calculated enthalpy of mixing curve at 1973 K with the experimental data of [28] is shown in Fig. 2. Even though the experimental enthalpy of mixing data reported by Batalin et al. [28] suggest that the maximum short range ordering should be around 20 at.% Y, this was impossible to obtain while maintaining the consistency with the other thermodynamic and phase diagram information of the system. The current thermodynamic calculation showed that the maximum short range ordering should be around 40 at.% Y. Near this composition, the Ni_2Y compound which has the most negative enthalpy of formation (−33.9 kJ/mol atom) occurs. Usually short range ordering is expected around the composition of the most stable compound. Besides, this calculation shows an improvement on the SGTE database [55] as shown in Fig. 2. Also, the entropy of mixing curve of the SGTE database [55] shows negative deviation which is unusual. This is corrected in the current work as shown in Fig. 3.

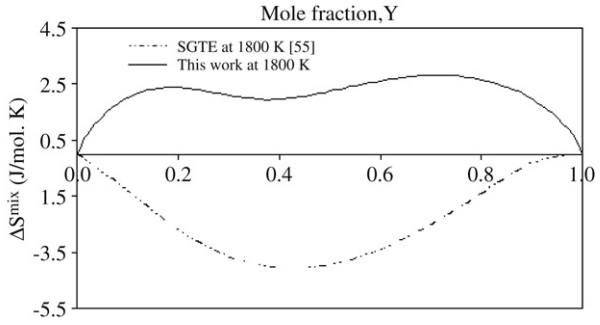

Fig. 3. Calculated entropy of mixing of liquid Ni–Y at 1800 K.

The calculated enthalpy of formation of the intermetallic compounds at 973 K with the experimental data of Subramanian and Smith [15] is shown in Fig. 4. Also, this calculation is compared with the predicted enthalpy of formation values by Mal et al. [25]. The calculated enthalpy of formation of most of the compounds show higher negative values than those of Subramanian and Smith [15]. Producing the compounds with a

Table 3
Entropy of formation of the compounds in the Ni–Y system.

Phase	$-\Delta S$ (J/mol atom K) (298 K)	$-\Delta S$ (J/mol atom K) (923 K)	$-\Delta S$ (J/mol atom K) (887–1224 K) [15]
$Ni_{17}Y_2$	−2.01	0.79	0.88 ± 0.34
Ni_5Y	−1.20	1.42	1.48 ± 0.41
Ni_4Y	−0.62	1.89	1.61 ± 0.48
Ni_7Y_2	−0.63	1.81	1.59 ± 0.55
Ni_3Y	−0.76	1.59	1.70 ± 0.73
Ni_2Y	−0.11	1.98	2.51 ± 0.90
NiY	−0.78	0.79	5.14 ± 1.84
Ni_2Y_3	−0.08	1.17	6.77 ± 2.34
NiY_3	0.07	0.85	8.58 ± 5.26

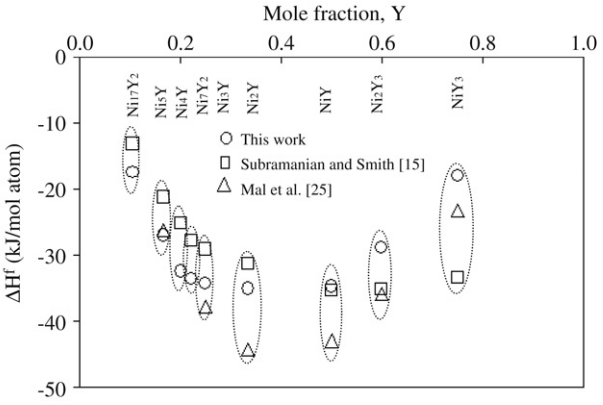

Fig. 4. Calculated enthalpy of formation of the intermetallic compounds in the Ni–Y system at 973 K.

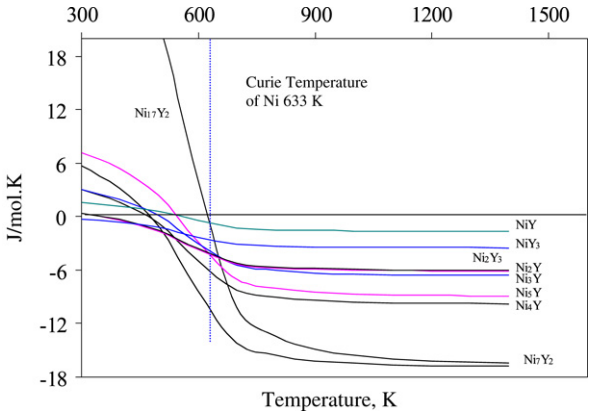

Fig. 5. Calculated entropy of formation of the Ni–Y compounds at different temperatures (the units for the entropy of formation are per mole of formula units instead of mol atom for clearer illustration).

less negative enthalpy of formation contradicted the experimental phase diagram information. Hence, higher negative values for the enthalpy of formation are used. The predicted values by Mal et al. [25] also show similar results as the present calculation.

It can be seen from Fig. 5 that the entropy of formation of the Ni–Y compounds decreases with temperature until around the Ni Curie temperature (633 K). Beyond this temperature, the entropy of formation approaches a constant value. This is due to the ferromagnetic nature of Ni. Subramanian and Smith [15] reported the entropy of formation of these compounds in the temperature range 887–1224 K as constant values. Table 3 lists the values obtained in this work in relation to those from [15]. It can be seen that satisfactory agreement was achieved for most of the compounds except those with high yttrium content. It is worth noting that Subramanian and Smith [15] reported high error limits for the entropy of formation of these compounds.

Table 4
Optimized model parameters of the Mg–Ni system.

Phase	Terms	a (J/mol atom)	b (J/mol atom K)
Liquid	Δg^0_{MgNi}	−16,829.43	5.02
	g^{Mg0}_{MgNi}	−15,864.18	10.49
	g^{0Ni}_{MgNi}	−16,345.55	1.26
Mg-hcp	${}^0L^{Mg\text{-}hcp}$	3,767.22	0
Ni-fcc	${}^0L^{Ni\text{-}fcc}$	36,835.04	0
Mg_2Ni	ΔG_f	−17,181.82	−0.4108
$MgNi_2$ $(Mg\%, Ni)_1$ $(Mg, Ni\%)_2$	${}^0G^{MgNi_2}_{Mg:Mg}$	8,333.33	12.66
	${}^0G^{MgNi_2}_{Mg:Ni}$	−21,944.04	5.76
	${}^0G^{MgNi_2}_{Ni:Mg}$	0.00	0.00
	${}^0G^{MgNi_2}_{Ni:Ni}$	5,466.66	6.73

The calculated Mg–Ni phase diagram in comparison with the available experimental data from the literature is shown in Fig. 6. There is a lack of experimental data for the liquidus curve in the region between Mg_2Ni and $MgNi_2$. Experiments in this region are necessary for a better assessment of this system. Nevertheless, the rest of the phase diagram shows very good agreement with the experimental data. The optimized parameters of the liquid and the intermetallic compounds are given in Table 4. A two sublattice model for the $MgNi_2$ as reported by Islam and Medraj [47] has been used to reproduce the homogeneity range of this phase.

The calculated integral enthalpy of mixing of the liquid at 1008 K is given in Fig. 7 which shows very good agreement with the experimental data of Feufel and Sommer [39]. The activity of liquid Mg and Ni calculated at 1100 K is shown in Fig. 8. The calculated activity of Mg shows a good agreement with the experimental data of Sryvalin et al. [40] and Micke and Ipser [32]. For the activity of Ni, however, not many experimental results are reported in the literature. The calculated activity of Ni shows good agreement with the data of Sryvalin et al. [40] who used the emf method to measure the activity. Also, a good agreement can be seen with the data of Sieben et al. [41] who measured the vapor pressure of Mg and calculated the activity of Ni using the Gibbs–Duhem equation.

The calculated enthalpy of formation at room temperature for Mg_2Ni and $MgNi_2$ compared with the available experimental data is shown in Fig. 9. The current results are in a very good agreement with Lukashenko and Eremenko [44] who obtained these values using the emf method with a molten salt galvanic cell. Also, there is a reasonable agreement between the current work and Schmahl and Sieben [41] and King and Kleppa [43] who determined the enthalpy of formation by transportation vapor pressure technique and solution calorimetry method, respectively. The calculated enthalpy of formation of Mg_2Ni is not in a very good agreement with the data of Smith and Christian [42] who used the Knudsen effusion vapor method but it is decided to be consistent with the other three groups since they were consistent among themselves.

A self-consistent thermodynamic database for the Mg–Ni–Y system has been constructed by combining the thermodynamic descriptions of the three constituent binaries Mg–Ni, Ni–Y and

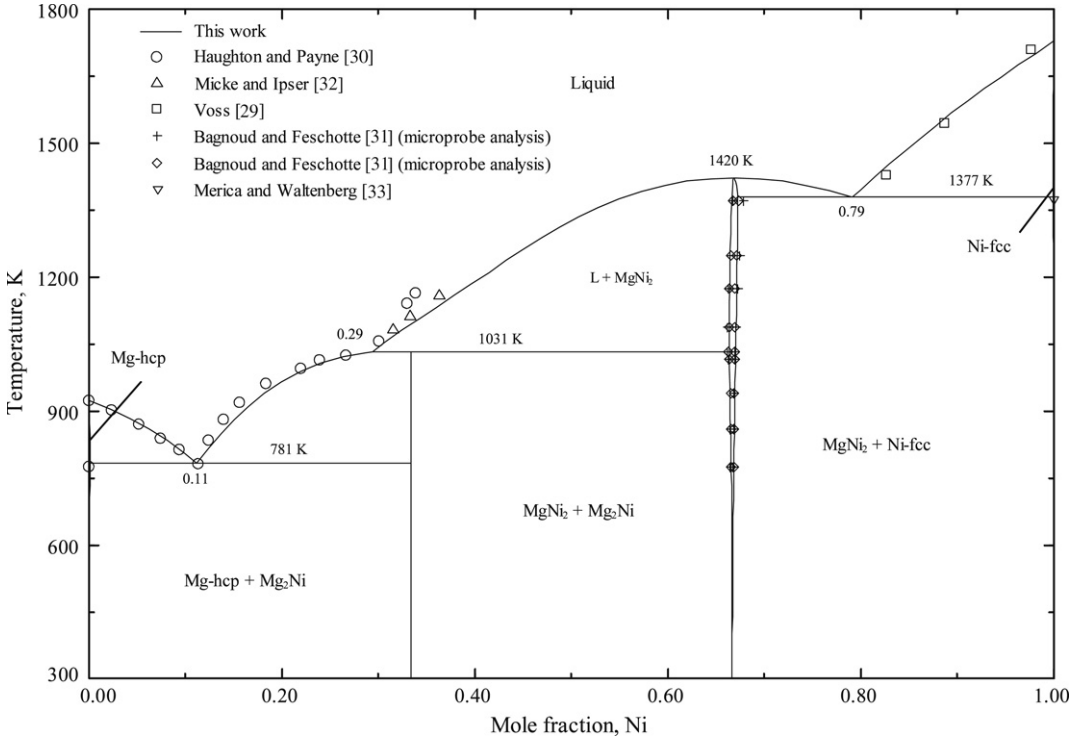

Fig. 6. Calculated Mg–Ni phase diagram.

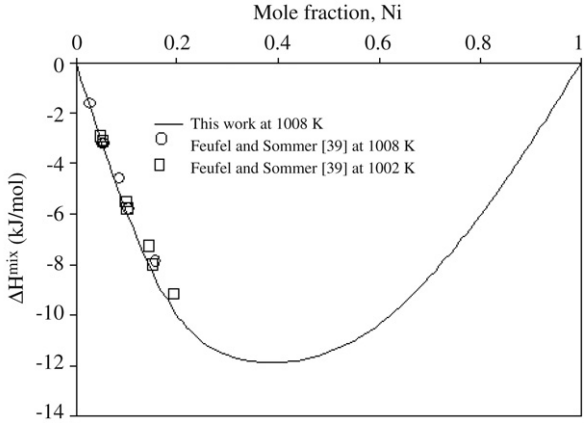

Fig. 7. Calculated enthalpy of mixing of liquid Mg–Ni at 1008 K.

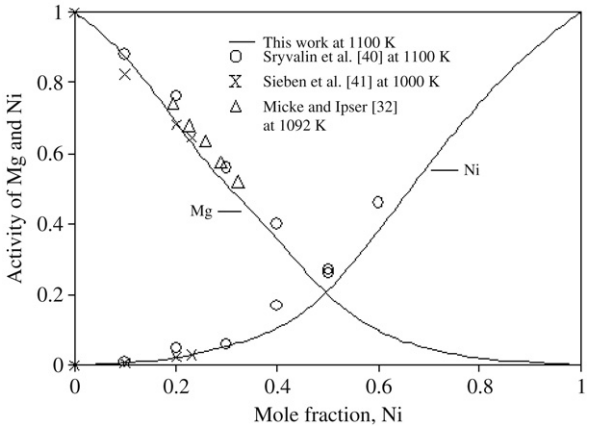

Fig. 8. Calculated activity of liquid Mg and Ni at 1100 K.

Mg–Y. According to Qiao et al. [56] if the excess thermodynamic properties in two of the three binary systems show similarity and significantly differ from the third one, the ternary system should be considered as an asymmetric system and the common component in the two similar binary systems should be chosen as the asymmetric component. The enthalpy of mixing curves of liquid Mg–Ni and Mg–Y showed similar maximum negative value (−10 and −8 kJ/mol, respectively) while they differed from Ni–Y (−26 kJ). Therefore, the Toop geometric model [9] with Mg as the asymmetric component has been used for the extrapolation to the ternary system. The two ternary compounds are included in the system by approximating their enthalpy of formation based on some indirect experimental information found in the literature since no direct experimental data could be found.

Aono et al. [52] used the casting method for the preparation of their sample for the investigation of the hydrogen absorption property of the $MgNi_4Y$ ternary compound. During their sample preparation a mixture of Ni_2Y and $MgNi_2$, total 3 gm, was compressed into a pellet and put inside a high-purity Mo crucible. The sample was then melted in an electric furnace at 1573 K. Although it is not mentioned how precise the temperature detection was and whether the Mo crucible reacted with the sample or not, this value is considered a higher end of the melting temperature of $MgNi_4Y$. Especially because they most likely used a little higher temperature to ensure complete melting of the sample. Therefore, it is decided to fix the melting temperature of this compound at 1552 K which can be seen in Fig. 10. This figure shows a vertical section in the Mg–Ni–Y system where the $MgNi_4Y$ melts congruently at a temperature close to that reported by [52].

On the other hand Kadir et al. [49] prepared a sample very rich of the Mg_2Ni_9Ycompound using an arc-melting furnace. Hence it is not possible to detect the melting point of this compound from this experiment. However they used annealing at 1271 K to prepare their sample which reveals that the melting temperature of this ternary compound should be higher than this temperature. Aono et al. [52] used a heat treatment temperature of 1423 K during their sample preparation for studying $MgNi_4Y$ which is about 150 K

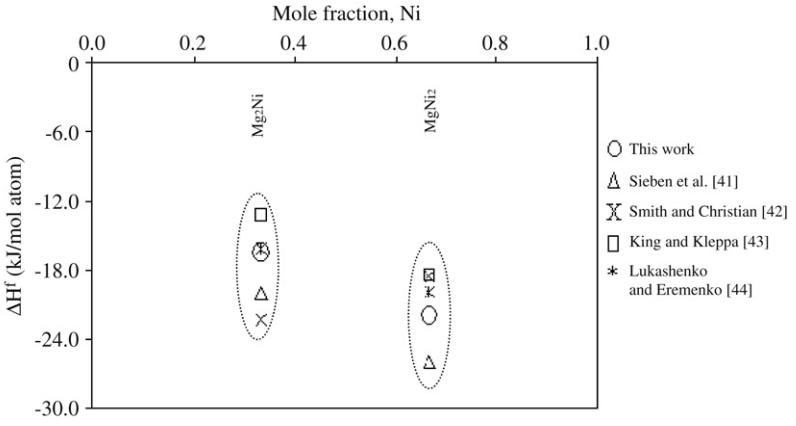

Fig. 9. Enthalpy of formation of the intermetallic compounds in the Mg–Ni system.

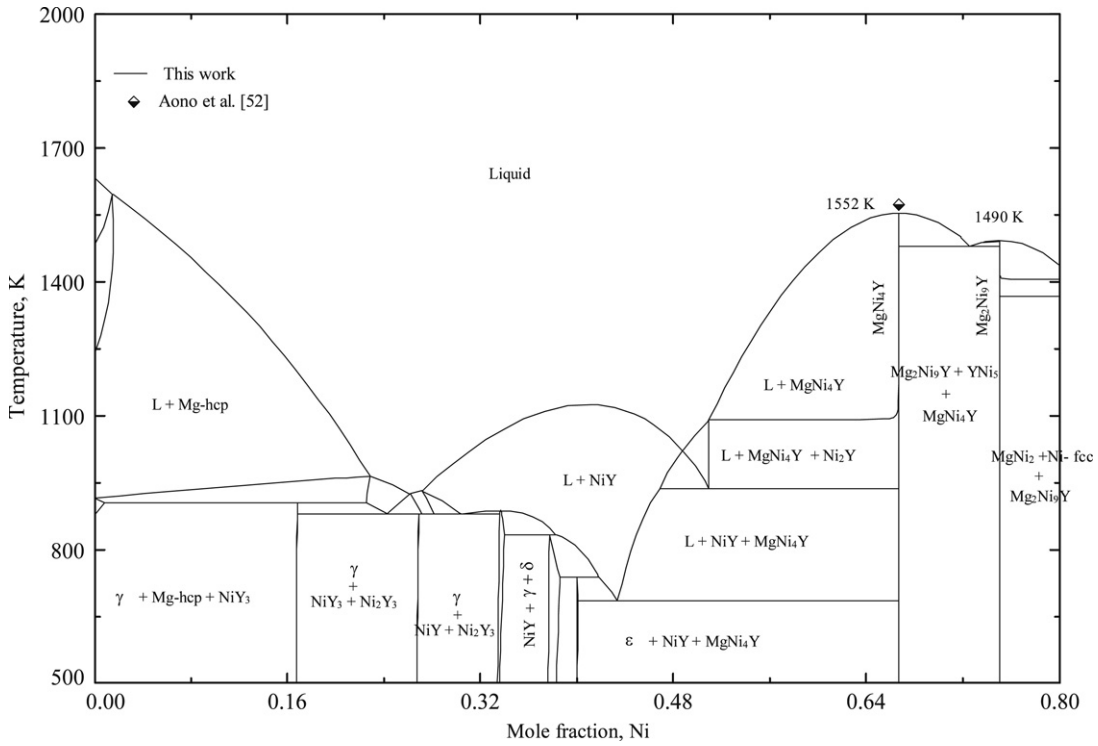

Fig. 10. A vertical section of the Mg–Ni–Y system showing the melting temperature of the ternary compounds.

Table 5
Optimized model parameters of the ternary compounds.

Phase	Terms	a (J/mol atom)	b (J/mol atom K)
$MgNi_4Y$	ΔG_f	−32,842.63	0.69
Mg_2Ni_9Y	ΔG_f	−24,445.86	1.75

higher than what [49] used for Mg_2Ni_9Y This indicates that the melting temperature of the Mg_2Ni_9Y should be lower than that of $MgNi_4Y$. In the present calculation the melting temperature of Mg_2Ni_9Y is kept at 1490 K as can be seen in Fig. 10. The model parameters of the $MgNi_4Y$ and Mg_2Ni_9Y compounds are given in Table 5.

Fig. 11a shows the calculated isothermal section of the Mg–Ni–Y system at 673 K using the predicted melting temperature values of the two ternary compounds. This present calculation shows a reasonable agreement with the reported phase diagram by Yao et al. [48]. It is worth noting that the experiments of Yao et al. [48] were only in the Ni-rich region of the system which were used to predict the triangulations shown in Fig. 11b. By lowering the melting temperature of the $MgNi_4Y$ compound the isothermal section could be adjusted more precisely but it is decided to be consistent with a higher melting point since according to the experimental detail of Aono et al. [52] it is quite clear that the melting temperature should be near 1552 K.

One of the triangulations in Fig. 11b, reported by Yao et al. [48] is between $MgNi_4Y$, Mg and Ni_2Y while in the present work in Fig. 11a, this is found to be between $MgNi_4Y$, $\varepsilon(Mg_{24}Y_5)$ and NiY. This is because Yao et al. [48] did not consider the existence of the ε-phase in their work. Also, Ni_2Y is an incongruently melting compound which melts at a temperature very close to the peritectic point. Therefore, it is more expected that $MgNi_4Y$ forms triangulation with NiY which melts congruently rather than with Ni_2Y.

Hara et al. [1] prepared one alloy sample of the Mg–Ni–Y system using the casting method to test the suitability of this system for hydrogen storage. Their alloy is composed of 82.5 at.% Mg, 15.9 at.% Ni and 1.6 at.% Y, and was melted at 1123 K. The present calculation also shows that this composition is in the liquid state at this temperature.

Table 6
Calculated invariant points and their reactions in the Mg–Ni–Y system.

Reaction	Type	Temp. (K)	Y (at.%)	Mg (at.%)	Ni (at.%)
Liquid ⇆ hcp-Mg + ε + $MgNi_4Y$	E_1	740.77	10.35	76.87	12.78
Liquid ⇆ Mg_2Ni_9Y + $MgNi_2$ + Ni-fcc	E_2	1366.95	1.29	19.95	78.76
Liquid ⇆ ε + $MgNi_4Y$ + YNi	E_3	683.83	27.31	37.87	34.82
Liquid ⇆ γ + YNi + Ni_2Y_3	E_4	877.70	53.81	21.43	24.76
Liquid + Mg_2Ni⇆ $MgNi_4Y$ + Mg-hcp	U_1	745.00	5.54	82.35	12.11
Liquid + $MgNi_2$⇆ $MgNi_4Y$ + Mg_2Ni	U_2	1011.83	2.33	61.78	35.89
Liquid + Mg_2Ni_9Y⇆ $MgNi_2$ + $MgNi_4Y$	U_3	1287.60	4.98	40.64	54.38
Liquid + $Ni_{17}Y_2$⇆ Ni-fcc + Mg_2Ni_9Y	U_4	1437.75	4.81	10.84	84.35
Liquid + Ni_5Y⇆ Mg_2Ni_9Y + $Ni_{17}Y_2$	U_5	1462.53	6.63	10.92	82.45
Liquid + Ni_5Y⇆ $MgNi_4Y$ + Mg_2Ni_9Y	U_6	1480.46	10.49	17.62	71.89
Liquid + Ni_5Y⇆ $MgNi_4Y$ + Ni_4Y	U_7	1519.76	20.38	8.63	70.99
Liquid + Ni_4Y⇆ $MgNi_4Y$ + Ni_7Y_2	U_8	1491.12	23.12	7.45	69.43
Liquid + Ni_7Y_2⇆ $MgNi_4Y$ + Ni_3Y	U_9	1438.81	26.38	6.72	66.90
Liquid + Ni_3Y⇆ $MgNi_4Y$ + Ni_2Y	U_{10}	1311.36	31.23	6.60	62.17
Liquid + Ni_2Y⇆ $MgNi_4Y$ + NiY	U_{11}	935.32	32.20	21.85	45.95
Liquid + δ ⇆ ε + NiY	U_{12}	736.22	30.21	39.12	30.67
Liquid + γ ⇆ δ + NiY	U_{13}	831.623	39.86	35.15	24.99
Liquid + Y_3Ni ⇆ γ + Ni_2Y_3	U_{14}	879.51	55.50	20.42	24.08
Liquid + hcp-Y ⇆ NiY_3 + γ	U_{15}	904.56	57.35	20.90	21.75
Liquid + β-Y ⇆ hcp-Y + γ	U_{16}	1038.43	56.75	29.68	13.57
Liquid ⇆ ε + $MgNi_4Y$	m_1	760.10	17.79	54.72	27.50
Liquid ⇆ $MgNi_2$ + Mg_2Ni_9Y	m_2	1397.05	2.40	28.37	69.23
Liquid ⇆ Ni_5Y + Mg_2Ni_9Y	m_3	1490.98	9.00	15.33	75.67
Liquid ⇆ Ni_5Y + $MgNi_4Y$	m_4	1537.26	16.67	11.88	71.45
Liquid ⇆ γ + YNi	m_5	886.24	49.56	25.27	25.17

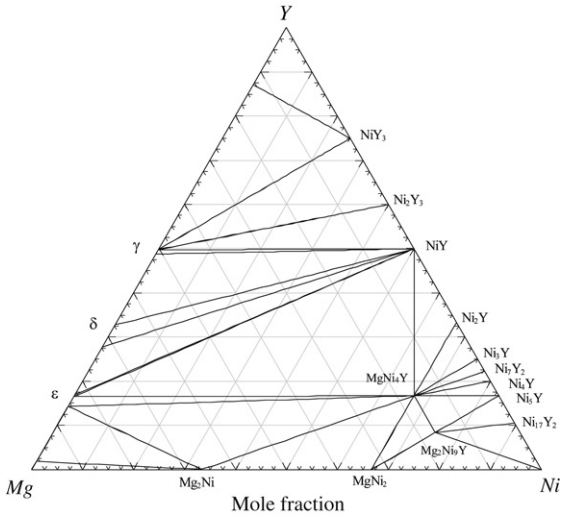

Fig. 11a. Calculated isothermal section of the Mg–Ni–Y system at 673 K.

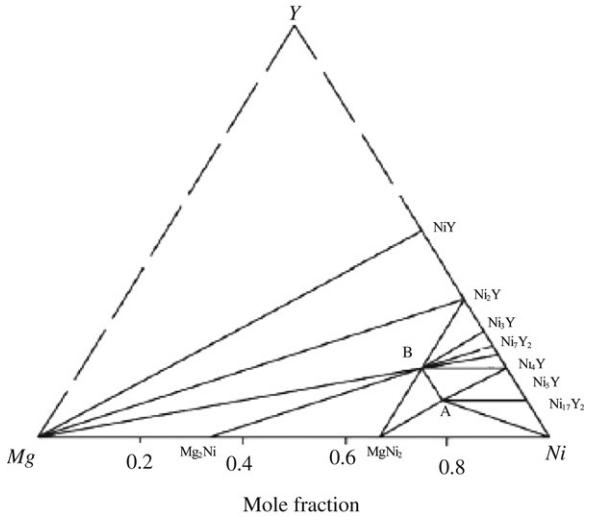

Fig. 11b. Isothermal section of the Mg–Ni–Y system at 673 K (Ni-rich part) (A) Mg_2Ni_9Y; (B) $MgNi_4Y$ [48].

All this information has been taken into consideration during the optimization of this system. No ternary interaction parameter is added during the process. The liquidus projection of the Mg–Ni–Y system is shown in Fig. 12. The univariant valleys are shown by the heavier lines and the arrows on these lines indicate the directions of decreasing temperature. There are four ternary eutectic points (E_1 to E_4), sixteen ternary quasi-peritectic points (U_1 to U_{16}) and five maximum or saddle points (m_1 to m_5) present in this system. A summary of all the reactions at these invariant points is given in Table 6.

5. Conclusion

A self-consistent thermodynamic database for the Mg–Ni–Y system has been constructed by combining the thermodynamic descriptions of the binaries Mg–Ni, Ni–Y and Mg–Y using the Toop geometric model. No ternary interaction parameter has been used for the extrapolation. Among the three binaries, Mg–Ni and Ni–Y systems have been optimized in this work using the modified quasichemical model for the liquid phase in order to consider the presence of the short range ordering. The optimized parameters for the Mg–Y system using the same model have been taken from a previous work by the same authors. The phase diagrams and the thermodynamic properties of all the binaries show a good agreement with the experimental data. More experimental investigation is required to obtain detailed information regarding the two ternary compounds ($MgNi_4Y$ and Mg_2Ni_9Y). The melting temperatures of these two compounds should be determined experimentally which is very important to establish a more accurate assessment of the Mg–Ni–Y system. Also, all the predicted invariant points are to be verified experimentally. The present work can be used to design key experiments for further verification of this system.

Acknowledgments

This research was carried out with the support of an NSERC Discovery Grant, Canada. The authors wish to express their appreciation for this support.

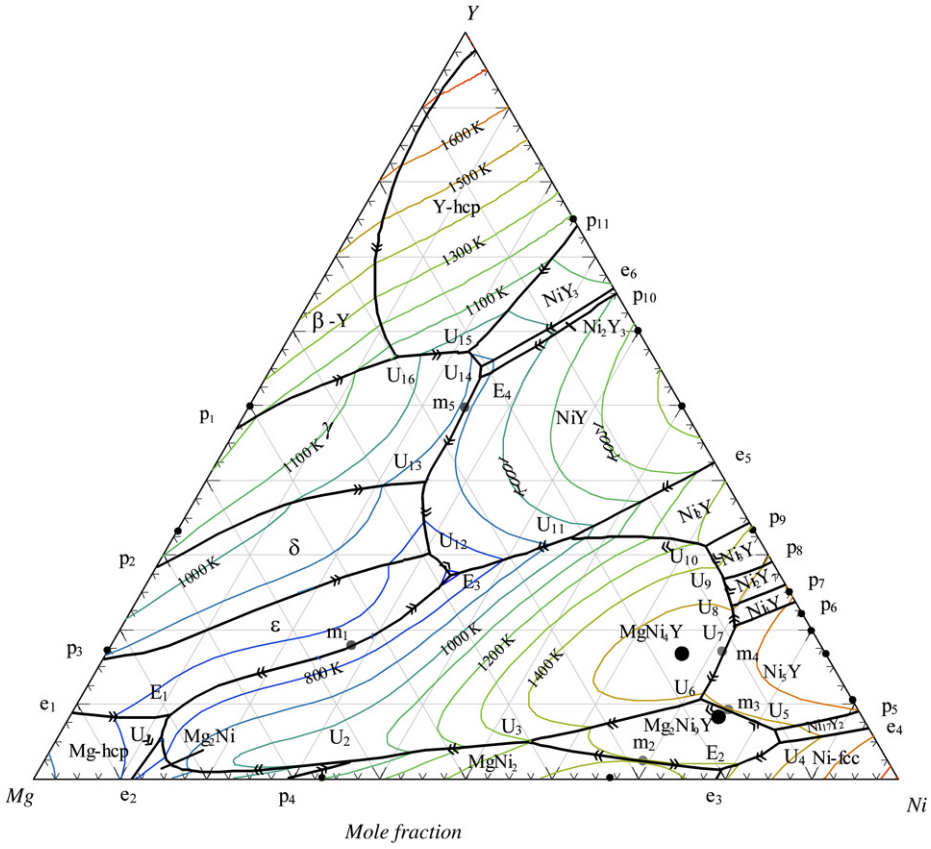

Fig. 12. Liquidus projection of the Mg–Ni–Y system.

References

[1] M. Hara, S. Morozumi, K. Watanabe, J. Alloys Compounds 414 (2006) 207–214.
[2] N. Cui, J.L. Luo, K.T. Chuang, J. Alloys Compounds 302 (2000) 218–226.
[3] G. Friedlmeier, M. Arakawa, T. Hirai, E. Akiba, J. Alloys Compounds 292 (1999) 107–117.
[4] Q.F. Li, K.Q. Qiu, X. Yang, Y.L. Ren, X.G. Yuan, T. Zhang, Mater. Sci. Eng. A 491 (2008) 420–424.
[5] A.D. Pelton, S.A. Degterov, G. Eriksson, C. Robelin, Y. Dessureault, Metall. Mater. Trans. B 31 (2000) 651–659.
[6] P. Chartrand, A.D. Pelton, Metall. Mater. Trans. A 32 (2001) 1397–1407.
[7] A.D. Pelton, P. Chartrand, G. Eriksson, Metall. Mater. Trans. A 32 (2001) 1409–1416.
[8] M. Mezbahul-Islam, D. Kevorkov, M. Medraj, J. Chem. Thermodynamic. 40 (7) (2008) 1064–1076.
[9] G.W. Toop, Trans. Amer. Inst. Min. 233 (5) (1965) 850–855.
[10] B.J. Beaudry, A.H. Daane, Trans. Met. Soc. AIME 218 (1960) 854–859.
[11] R.F. Domagala, J.J. Rausch, D.W. Levinson, Trans. Am. Soc. Met. 53 (1961) 137–155.
[12] K.H.J. Buschow, Rep. Progr. Phys. 40 (10) (1977) 1179–1256.
[13] K.H.J. Buschow, J. Less-Common Met. 11 (3) (1966) 204–208.
[14] P. Nash, Binary Alloy Phase Diagrams, 2nd ed., ASM International, Materials Park, OH, 1991, p. 2885.
[15] P.R. Subramanian, J.F. Smith, Metall. Trans. B 16 (3) (1985) 577–584.
[16] Z. Du, W. Zhang, J. Alloys Compounds 245 (1996) 164–167.
[17] N. Mattern, M. Zinkevich, W. Loser, G. Behr, J. Acker, J. Phase Equilib. Diffus. 29 (2) (2008) 141–155.
[18] Y.Y. Pan, P. Nash, Binary Alloy Phase Diagrams, 2nd ed., ASM International, Materials Park, OH, 1991, pp. 2406–2408.
[19] M. Palumbo, G. Borzone, S. Delsante, N. Parodi, G. Cacciamani, R. Ferro, L. Battezzati, M. Baricco, Intermetallics 12 (2004) 1367–1372.
[20] P. Nash, Bull. Alloy Phase Diagrams 10 (2) (1989) 129–132.
[21] Z. Huaiying, O. Xiangli, Z. Xiaping, J. Alloys Compounds 177 (1) (1991) 101–106.
[22] Y.Y. Pan, P. Nash, Binary Alloy Phase Diagrams, 2nd ed., ASM International, Materials Park, OH, 1991, p. 77.
[23] D. Gignoux, D. Givord, R. Lemaire, A.N. Saada, A.D. Moral, J. Magn. Magn. Mater. 23 (3) (1981) 274–278.
[24] D. Gignoux, D. Givord, A. Lienard, J. Appl. Phys. 53 (3) (1982) 2321–2323.
[25] H.H.V. Mal, K.H.J. Buschow, A.R. Miedema, J. Less-Common Met. 49 (1976) 473–475.
[26] A.R. Miedema, J. Less-Common Met. 46 (1) (1976) 67–83.
[27] R.E. Watson, L.H. Bennett, Calphad 8 (4) (1984) 307–321.
[28] G.I. Batalin, V.A. Stukalo, N. Neshchimenko, V.A. Gladkikh, O.I. Lyuborets, Izv. Akad. Nauk SSSR, Metall. (6) (1977) 44–45.
[29] G. Voss, Z. Anorg. Chem. (57) (1908) 34–71.
[30] J.L. Haughton, R.J. Payne, J. Inst. Met. 54 (1934) 275–283.
[31] P. Bagnoud, P. Feschotte, Z. Metallkd. 69 (1978) 114–120.
[32] K. Micke, H. Ipser, Monatsh. Chem. 127 (1996) 7–13.
[33] P.D. Merica, R.G. Waltenberg, Tech. Paper, Nat. Bureau Stand. (US) 19 (1925) 155–182.
[34] J.S. Wollam, W.E. Wallace, J. Phys. Chem. Solids 13 (1960) 212–220.
[35] K.H.J. Buschow, Solid State Commun. 17 (1975) 891–893.
[36] F. Laves, H. Witte, Metallwirtschaft, Metaltech 14 (1935) 1001–1002.
[37] K.H. Lieser, H. Witte, Z. Mettalkd. 43 (1952) 396–401.
[38] K. Schubert, K. Anderko, Z. Mettalkd. 42 (11) (1951) 321–324.
[39] H. Feufel, F. Sommer, J. Alloys Compounds 224 (1995) 42–54.
[40] I.T. Sryvalin, O.A. Esin, B.M. Lepinskikh, J. Phys. Chem. 38 (5) (1964) 637–641.
[41] P. Sieben, N.G. Schmahl, T.B. Giesserei, Giesserei 18 (4) (1966) 197–211.
[42] J.F. Smith, J.L. Christian, Acta Metall. 8 (1960) 249–255.
[43] R.C. King, O.J. Kleppa, Acta Metall. 12 (1964) 87–97.
[44] G.M. Lukashenko, V.N. Eremenko, Izv. Akad. Nauk SSSR Met. 3 (3) (1966) 161–164.
[45] A.A. Nayeb-Hashemi, J.B. Clark, Bull. Alloy Phase Diagr. 6 (3) (1985) 238–244.
[46] M.H.G. Jacobs, P.J. Spencer, Calphad 22 (4) (1998) 513–525.
[47] F. Islam, M. Medraj, Calphad 29 (2005) 289–302.
[48] Q. Yao, H. Zhou, Z. Wang, J. Alloys Compounds 421 (2006) 117–119.
[49] K. Kadir, T. Sakai, I. Uehara, J. Alloys Compounds 257 (1997) 115–121.
[50] K. Kadir, T. Sakai, I. Uehara, J. Alloys Compounds 287 (1999) 264–270.
[51] K. Kadir, D. Noreus, I. Yamashita, J. Alloys Compounds 345 (2002) 140–143.
[52] K. Aono, S. Orimo, H. Fujii, J. Alloys Compounds 309 (2000) L1–L4.
[53] A.T. Dinsdale, Calphad 15 (1991) 317–425.
[54] Factsage 5.4.1, Thermfact (Centre for Research in Computational Thermochemistry), Montreal, QC, Canada, 2006.
[55] W. Martienssen, (Editor in Chief) Lehrstuhl fur Werkstoffchemie (Ed.), Rheinisch-Westf˙alische Technische Hochschule Aachen, Thermodynamic Properties of Inorganic Materials compiled by SGTE, Scientific Group Thermodata Europe, 4/19B4, 2006, pp. 123-126.
[56] Z.Y. Qiao, X. Xing, M. Peng, J. Phase Equilib. 17 (6) (1996) 502–507.